



PV Inverters and Modulation Strategies: A Review and A Proposed Control Strategy for Frequency and Voltage Regulation

Shayan Ebrahimi¹, Ali Moghassemi¹, Javad Olamaei^{1*}

¹ Department of Electrical Engineering, South Tehran Branch, Islamic Azad University, Tehran, Iran.

Received: 09-Sep-2019, Revised: 16-Dec-2019, Accepted: 22-Dec-2019.

Abstract

To ensure the reliable delivery of AC power to consumers from renewable energy sources, the photovoltaic inverter has to ensure that the frequency and magnitude of the generated AC voltage are within acceptable limits. This paper develops models and control strategies for the DC-AC converter to ensure that the sinusoidal waveform of the desired frequency voltage and magnitude generated for both single-phase and three-phase operation depend on the robustness of the inverter control system. The paper reviews various topologies and modulation approaches for photovoltaic inverters in both single-phase and three-phase operational modes. Finally, a proposed control strategy is presented to ensure frequency and voltage regulation.

Keywords: Voltage Regulation, Frequency Regulation, PV Inverter, Harmonic Reduction.

1. INTRODUCTION

The photovoltaic (PV) inverter is the key power electronic interface for both the on-grid (grid-connected) and off-grid (stand-alone) PV power systems. It has the main function of converting the DC power generated by the PV array into grid-synchronized AC power. To ensure reliable delivery of power to consumers from the renewable energy generator, the inverter has

to ensure that the frequency and magnitude of the generated voltage are within the acceptable limits. In any power system, this requirement, for the supply frequency, is necessary to be within a narrow band due to the following reasons [1]:

- It ensures that motor-based loads in both industrial and domestic applications operate at the required constant speeds. This is because of the fact that the speed

*Corresponding Authors Email:
j_olamaei@azad.ac.ir

of AC electrical drives is frequency sensitive.

- As a basis for timing various processes in electronic applications.
- For the safe operation of power transformers. Transformers are generally sensitive to frequent changes and maybe overloaded if the frequency drifts substantially from the nominal value.

Effective control of the magnitude and frequency of the AC output voltage requires a robust control technique. The PWM (pulse width modulation) technique is a popular method for achieving such an effective control, with the SPWM (sinusoidal PWM) variant being able to provide output voltages close to a sine wave by reducing the lower order harmonics to a negligible level [2-3]. In addition to controlling both the voltage magnitude and frequency, efficiency consideration has been a major driving factor of PV inverter technology due to the high cost of PV solar energy. Compared to motor drive inverters, PV inverters are more complex in both hardware and functionality. Such inverters, in addition to the primary function of DC-AC conversion, may also feature the following functionalities [4-5]: maximum power point tracking (MPPT); anti-islanding; for on-grid systems; grid synchronization; and data logging.

The main focus of this paper is the development of control algorithms that can effectively regulate the magnitude and frequency of the generated output AC voltage with minimal harmonics for PV power plants in the following modes of operation: single-phase operation; three-phase grid-connected operation; and three-phase standalone operation.

Firstly, a review of DC-AC converter interfaces classified according to their utilization topologies is done. This is followed by a review of such converters based on their schematic topologies. Thirdly, a review of the popular modulating strategies for DC-AC conversion used in single-phase applications is done. This is followed by a review of the vector control scheme applied for the control of a three-phase PV power plant in both the grid-connected mode and in a standalone mode. Finally, the simulation results and discussions are presented, followed by the paper conclusions.

2. REVIEW OF INVERTER TOPOLOGIES FOR PV SYSTEMS

To decrease the cost and increase the efficiency of PV systems, many inverter utilization topologies have been developed. Four of most popular of these topologies are discussed below [4-6].

Centralized Inverter Topology: In this topology, Fig. 1(a), the PV modules are connected in series and parallel to achieve a higher power – typical unit sizes range 100 – 1000 kW with three-phase topology. One common central inverter connected to the common DC bus is used to achieve this higher power. Despite the advantage of not requiring pre-inverter voltage boost converter because of use of series-connected strings to achieve high voltages, this topology has the following disadvantages [6]: power losses due to mismatch between PV modules; losses in string diodes; losses due to common MPPT; use of high voltage DC cables between PV panels and inverter; and limited system reliability due to dependence on a

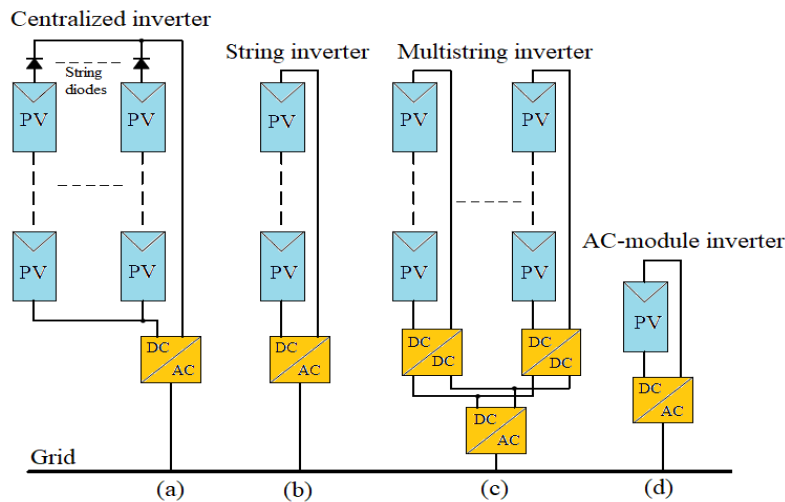


Fig. 1. PV systems configurations: (a) centralized, (b) string, (c) multi-string, and (f) module integrated.

single inverter – failure of which throws the entire plant out of operation.

String Inverter Topology: In this topology, Fig. 1(b), the PV plant is divided into several parallel strings which each string has a separate inverter. These string inverters are paralleled and connected to the grid (or the AC bus for off-grid systems). Each of these string inverters is equipped with MPPT capability to increase the energy yield by the mitigation of PV mismatch and shading losses. The advantages of this topology include [6-7]: use of fewer PV panels since DC-DC converters can easily be incorporated to boost the string voltage; no losses in the string diodes; and enhanced supply reliability due to dependence on more than one inverter. This topology has evolved as the standard for grid-connected PV systems for lower power applications ranging from 0.4 – 2 kW, especially for small roof-top plants.

Multi-string Inverter Topology: This topology, Fig. 1(c), is a derivative of the

string topology used for higher power applications – typically in the 1.5 – 5.6 kW range for medium-large roof-top plants. Each string is equipped with a separate DC-DC converter integrated with MPPT capability. These strings with the DC-DC converters and MPPT functionalities are then paralleled through a common DC-AC inverter. The unique advantages of this topology include [6-7]: compactness and cost-competitiveness; combines advantages of central and string topologies; and ability to incorporate PV strings of different technologies and different orientations.

Module Integrated Inverter Topology: In this topology, Fig. 1(d), a single PV module is directly connected to the grid via its integrated inverter with MPPT functionality. The advantages of this topology include [6-7]: reduced mismatch losses; better optimization of power extraction due to separate MPPT; and modularity of usage because of the plug-and-play nature. However, it has the following demerits [6]:

low efficiency occasioned by boosting of the low DC voltage of the panel to a higher level needed by the inverter; low power conversion, and limited to low wattage applications – just one panel integrated.

3. REVIEW OF INVERTER SCHEMATIC TOPOLOGIES FOR PV SYSTEMS

New innovative topologies have recently been developed for PV inverters. The primary driving factor is increasing the system's efficiency. Other considerations include cost reductions and increasing the system's lifetime. Efficiency improvement (of between 1 – 2 %) has been achieved by the elimination of galvanic isolation provided by integration of either high frequency (HF) transformer in the boost converter section or low frequency (LF) transformer in the output section [2]. While the transformerless PV inverter topologies offer advantages: improved efficiency; lower manufacturing cost and size and mass reductions, they introduce the following issues to the system [8-10]:

- No galvanic isolation between the AC and DC sections of the inverter associated with safety issues in fault situations.
- DC current injection into the AC network with the negative consequences of the poor performance of the grid system.
- PV array voltage fluctuation due to capacitive leakage currents arising from the sandwich structure of a PV panel developing a capacitance to earth with safety and EMC issues.

Modern inverter topologies have tried to address these issues of efficiency and safety using the following two well-known converter topologies [3-4, 10]:

H-bridge or Full-bridge: This is the basic circuit used to synthesize AC power from DC power by sequential opening and closing of the power switches. Fig. 2 shows the basic full-bridge topology with integrated PV arrays as the DC source. The output voltage of the topology can take various levels ($+V_{dc}$, 0, $-V_{dc}$) depending on the sequence of closing the switches [11]. The normal switching sequence of this topology is shown in Table 1.

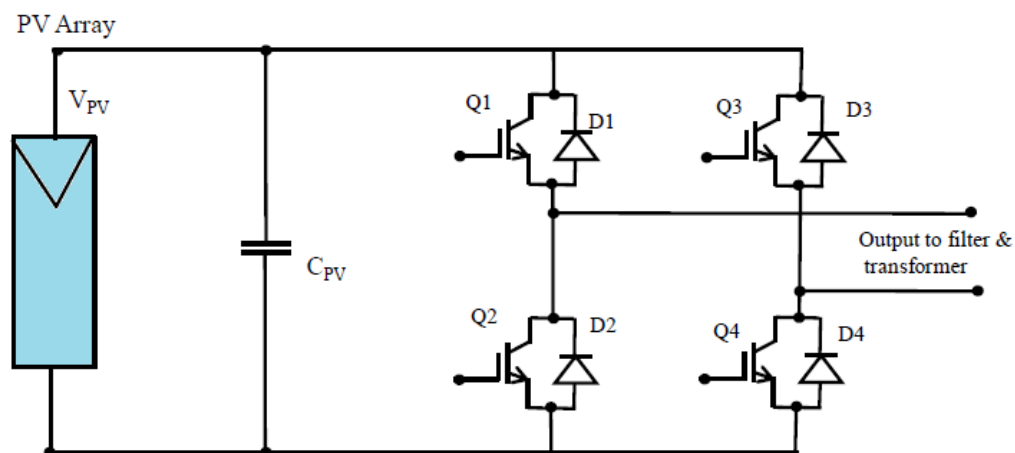


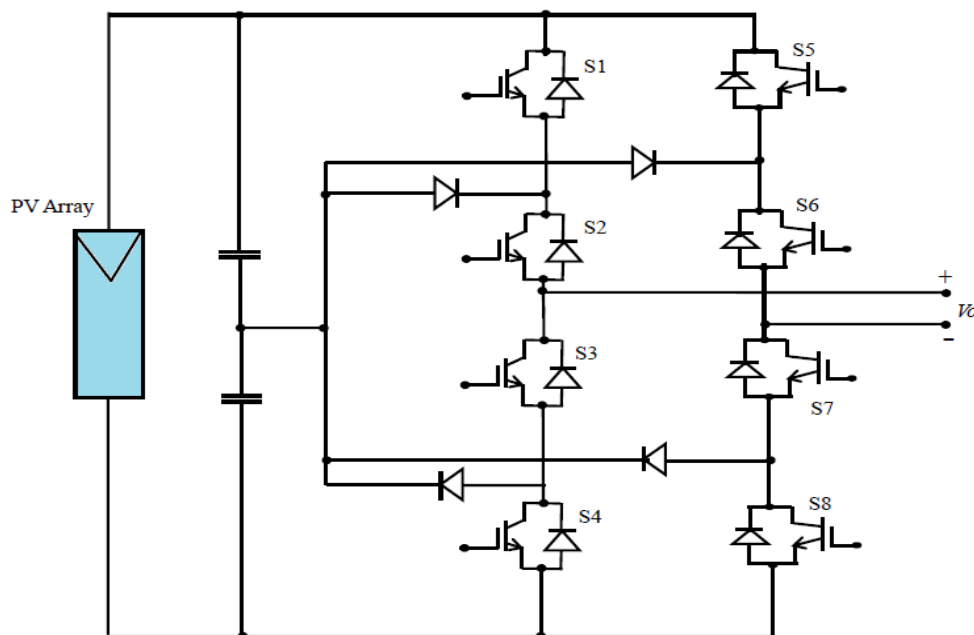
Fig. 2. Basic H-bridge or full-bridge inverter with integrated PV array.

Table 1. Switching sequence for the H-bridge topology.

Switch Sequence	Output Voltage Level
Q_1 & Q_4 closed	$+V_{PV}$
Q_3 & Q_2 closed	$-V_{PV}$
Q_1 & Q_3 closed	0
Q_2 & Q_4 closed	0

Multilevel inverter topology: The multilevel inverter approach uses an aggregation of H-bridges to produce additional voltage levels [1, 11]. The production of these voltage levels results in a staircase waveform that closely approaches a sinusoid. Multilevel inverters are becoming popular in medium and high-power inverter applications for interfacing renewable energy to the grid. Fig. 3 is a diode clamped type of multilevel inverter topology. A brief discussion of some modern derivatives of these two topologies is presented in the following section.

3.1. Transformerless Topologies

**Fig. 3. A diode-clamped multilevel inverter topology.**

This section presents the key operational features of some high-tech transformerless PV inverter structures that have addressed the shortcomings of the transformerless designs discussed earlier. They are all derivatives of the basic H-bridge topology.

3.1.1. H5 Inverter Topology

This topology is a classical H-bridge with an integrated extra fifth switch (hence the name) in the positive bus of the dc-link [5, 10] as shown in Fig. 4.

The switching scheme is based on the hybrid method, which is a variant of the unipolar scheme (explained in section 4.2). With this switching scheme, Q_5 , Q_4 & Q_2 are switched at high frequency while Q_1 & Q_3 are switched at the grid frequency. Two zero output voltages are available when Q_5 is *OFF*, and Q_1 & Q_3 are *ON*. The details of the switching states are shown in Table 2. The

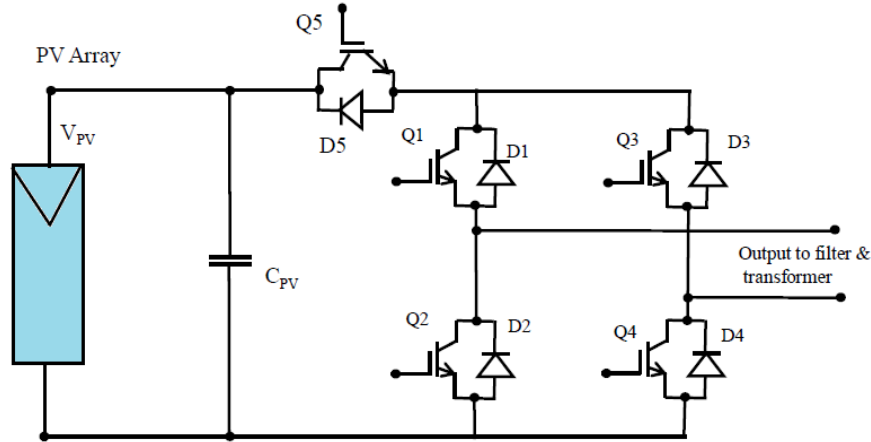


Fig. 4. H5 inverter topology with integrated PV array.

Table 2. Switching states for H5 inverter topology.

Switching State	Switches ON	Switched OFF	Output Voltage
1	Q_1, Q_4, Q_5	Q_2, Q_3	$+V_{dc}$
2	Q_1	Q_2, Q_3, Q_4, Q_5	0
3	Q_2, Q_3, Q_5	Q_1, Q_4	$-V_{dc}$
4	Q_3	Q_1, Q_2, Q_4, Q_5	0

inclusion of the extra fifth switch, Q_5 , helps to achieve the following [5, 9]: isolation of the PV array from the grid during zero voltage state; and avoidance of DC current injection into the grid during the zero-voltage state. The H5 topology has the following advantages [5, 9]: the use of three-level modulation ($+V_{dc}$, 0, $-V_{dc}$) yields lower core losses; a higher efficiency of up to 98 % due to no DC current injection during the zero-voltage state; and low leakage current and low electromagnetic interference (EMI).

Despite these advantages, it has the disadvantage of a higher switch count because of the use of an extra switch. However, since the H5 topology isolates the PV panels from the grid during zero-voltage state using the extra switch; possesses high efficiency; and has low leakage current and low EMI, it is very suitable for use in transformerless PV applications [5, 9, 10].

3.1.2 HERIC Inverter Topology

This topology is a derivative of the classical H-bridge. The HERIC (highly efficient and reliable inverter concept) topology incorporates a bypass leg in the AC side of the H-bridge topology using two back-to-back IGBT switches, as shown in Fig. 5. The AC bypass provides the following functionality [8-10]: isolation of the PV array from the grid during zero voltage state; and avoidance of DC current injection into the grid during the zero-voltage state.

The switching scheme is: Q_1, Q_4 and Q_2, Q_3 are switched at high-frequency while Q_5 and Q_6 are switched at the grid frequency. The details of the switching states are shown in Table 3. While having the drawback of high switch count because of the inclusion of the two extra switches, the HERIC topology has the following advantages [8-10]: lower

core losses because of unipolar operation; decouples the PV array from the grid during zero-voltage state on the AC side; high efficiency of up to 97 % due to no current injection during zero-voltage state; and low leakage current and low EMI. These advantages make the HERIC topology very suitable for use in transformerless PV applications.

3.1.3 Other Transformerless Topologies

Other high-tech transformerless topologies for PV that try to overcome the shortcomings of non-inclusion of a transformer, discussed earlier, include [5, 8-10]:

- The REFU Inverter. This is a derivative of the classical H-bridge topology.
- The Full-Bridge Zero Voltage Rectifier (FB-ZVR), which is a derivative of the HERIC topology.
- Neutral Point Clamped (NPC) Half-Bridge Inverter.

4. REVIEW OF MODULATION STRATEGIES FOR DC/AC CONVERSION

The PWM is the most popular modulation strategy that optimizes the PV inverter circuit operation for both single-phase and three-phase operations [3]. This technique controls each power switch by comparing a sinusoidal reference wave with a triangular carrier wave and producing an output voltage having a fundamental frequency of the same value as the reference waveform [2, 5]. The amplitude of the output is also dependent on the relative amplitudes of the reference and the carrier signals. The three variants of PWM techniques used for the optimization of PV inverters based on the popular H-bridge topology and their derivatives are briefly reviewed in the following subsections.

4.1. Bipolar (BP) Switching Scheme

The bipolar switching scheme, illustrated in Fig. 6, is based on the synchronization of a sinusoidal reference signal with a triangular carrier signal.

The instantaneous value of the sine reference (v_{sine}) is compared with the triangular carrier ($v_{triangle}$) to generate the output voltage. Mathematically, the operating principle is [2, 3]:

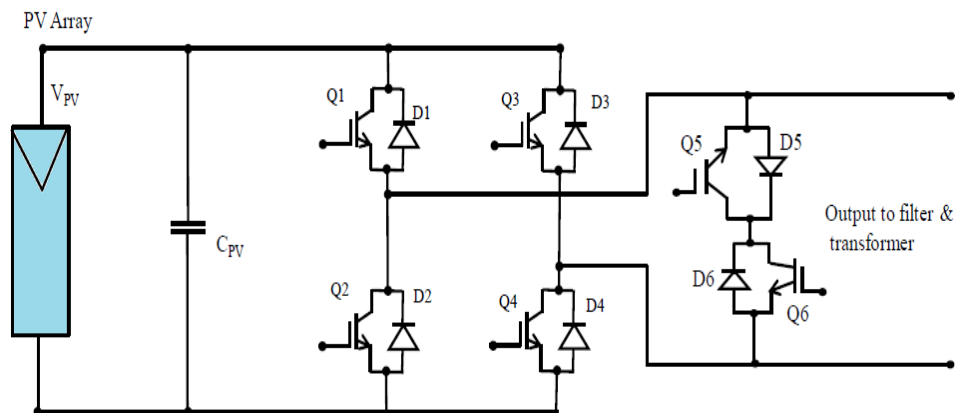
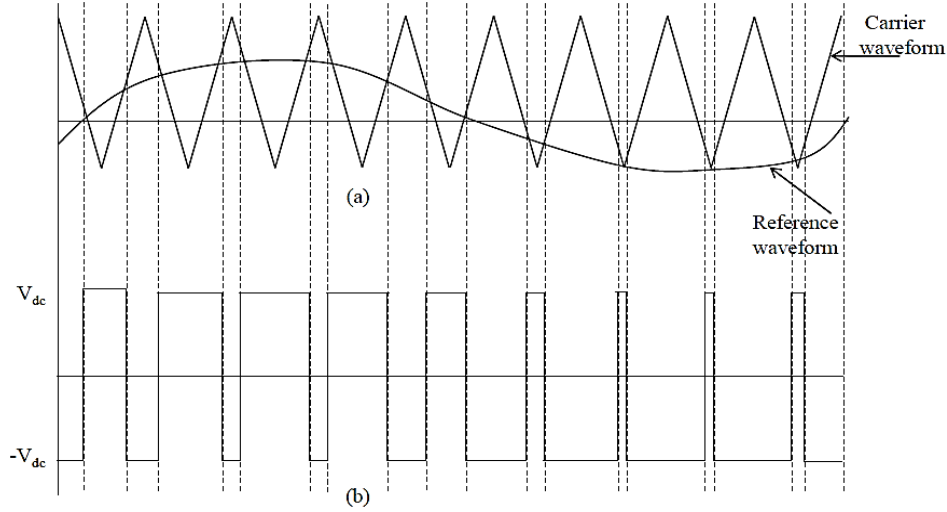


Fig. 5. HERIC inverter topology.

Table 3. Switching states for HERIC inverter topology.

Switching State	Switches ON	Switched OFF	Output Voltage
1	Q_1, Q_4, Q_6	Q_2, Q_3, Q_5	$+V_{dc}$
2	Q_6	Q_1, Q_2, Q_3, Q_4, Q_5	0
3	Q_2, Q_3, Q_5	Q_1, Q_4, Q_6	$-V_{dc}$
4	Q_5	Q_1, Q_2, Q_3, Q_4, Q_6	0

**Fig. 6. Bipolar PWM switching scheme.**

$$v_o = +V_{dc} \quad \text{for } v_{sine} > v_{triangle} \quad (1)$$

$$v_o = -V_{dc} \quad \text{for } v_{sine} < v_{triangle} \quad (2)$$

where, V_{dc} is the DC supply voltage and v_o is the output voltage. Thus, the output voltage alternates between two voltage levels ($+V_{dc}$ and $-V_{dc}$) as shown in Fig. 6(b). The term bipolar is because of the fact that this switching scheme alternates between plus and minus the DC supply voltage a two-level operation. The application of the bipolar switching scheme to the single-phase full-bridge topology is shown in Fig. 7 where the switching sequence is based on [2-3]:

$$Q_1 \text{ \& } Q_4 \text{ are ON} \quad \begin{matrix} v_{sine} > v_{triangle} \\ (v_o = +V_{dc}) \end{matrix} \quad (3)$$

$$Q_2 \text{ \& } Q_3 \text{ are ON} \quad \begin{matrix} v_{sine} < v_{triangle} \\ (v_o = -V_{dc}) \end{matrix} \quad (4)$$

While the power switches are turned ON diagonally, the switches of a switching leg must not be turned ON at the same time to avoid short-circuit across the DC source a condition known as shoot-through fault [3]. Inclusion of switching transition times, known as deadtime, is often used to avoid shoot-through occurrence [11].

4.2. Unipolar (UP) Switching Scheme

In a unipolar switching scheme, the inverter output voltage switches between three levels ($+V_{dc}$, 0, $-V_{dc}$) over a complete fundamental cycle. This is achieved by modulating the phase legs with 180 degrees opposed

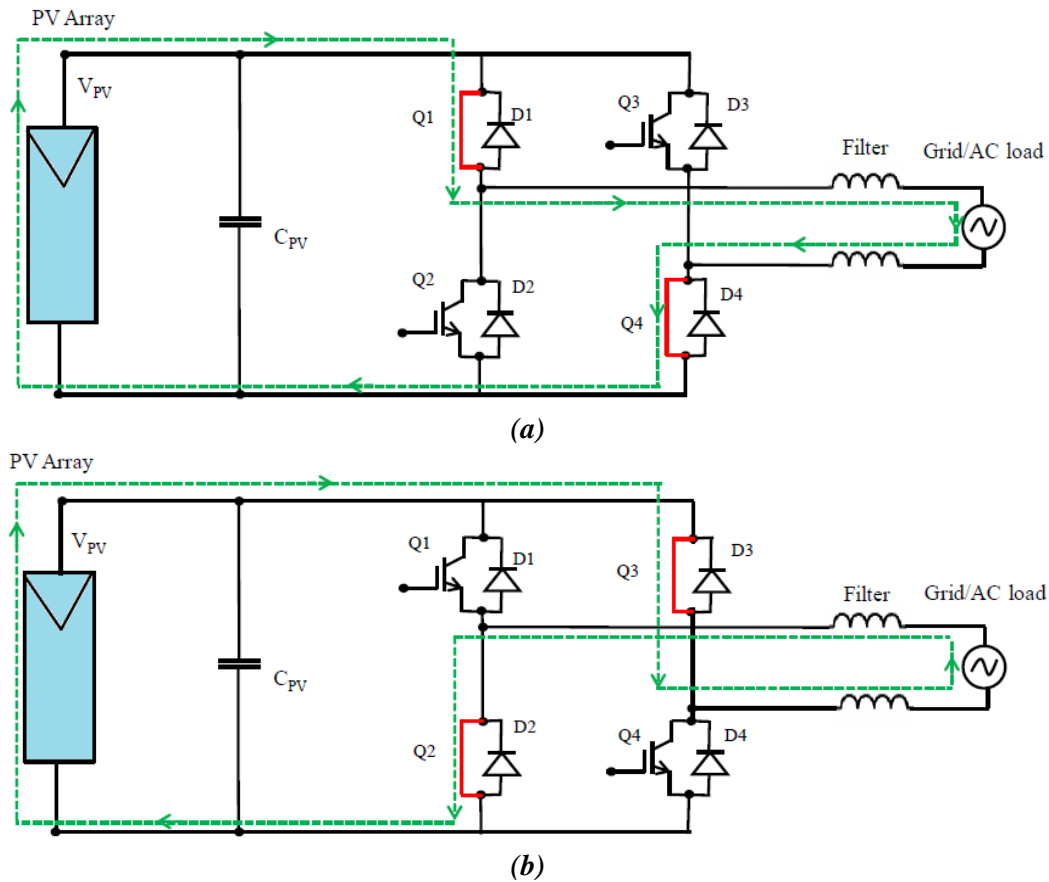


Fig. 7. Full-bridge topology with bipolar switching scheme: (a) Q_1 & Q_4 turned ON, and (b) Q_3 & Q_2 turned ON.

reference waveforms – that is, with a mirrored sinusoidal reference for each phase leg [3]. For the full-bridge topology, the switching states based on the unipolar switching scheme are shown in Table 4. The output voltage of the full-bridge inverter controlled with the unipolar switching scheme is given by [2]:

$$v_o(t) = V_{dc} \times M_a \times \sin\omega t + \text{harmonics} \quad (5)$$

where $\omega = 2\pi f$ is the frequency of the sine wave in radians per second and f is the frequency in Hz; M_a is the amplitude modulation index which is defined as the ratio of the peak of the sine waveform (v_{sine})

to that of the triangular waveform ($v_{triangle}$). From (5) it is clear that for the unipolar switching scheme, the peak of the fundamental component of the output voltage has a peak value proportional to the amplitude modulation index. In general, for the UP switching scheme, the frequency and magnitude of the output voltage are controlled by the reference sine wave, whereas the harmonic content of the output voltage depends on the frequency modulation index (M_f) defined as the ratio of the frequency of the triangular wave to that of the sine wave used for the modulation process [2-3].

Table 4. Switching states using unipolar switching scheme.

Switching State	Switches ON	Switched OFF	Output Voltage
1	Q_1, Q_4	Q_2, Q_3	$+V_{dc}$
2	Q_2, Q_4	Q_1, Q_3	0
3	Q_2, Q_3	Q_1, Q_4	$-V_{dc}$
4	Q_1, Q_3	Q_2, Q_4	0

4.3. Hybrid Switching Scheme

The hybrid switching scheme is a variant of the unipolar scheme in which one phase leg is switched at the grid low frequency while the other phase leg is switched at a high carrier frequency to generate the three output voltage levels ($+V_{dc}$, 0, $-V_{dc}$) [5]. Thus, it has two high-frequency switches and two low-frequency switches. Table 5 summarizes the advantages, disadvantages and limitations of these inverter modulation strategies with integrated H-bridge topology for transformerless PV applications [5, 8-10].

Table 5. Merits, demerits and limitations of modulation schemes.

Scheme	Bipolar	Unipolar	Hybrid
Merits	<ul style="list-style-type: none"> Very low leakage current Low EMI 	<ul style="list-style-type: none"> Lower filtering requirements Lower core losses due to three voltage levels produced. High efficiency of up to 98% due to reduced core losses during zero voltage states 	<ul style="list-style-type: none"> Lower core losses Higher efficiency, up to 98%
Demerits	<ul style="list-style-type: none"> Higher filtering requirements High core losses due to two voltage levels produced Lower efficiency 96.5% 	<ul style="list-style-type: none"> High leakage current High EMI 	<ul style="list-style-type: none"> Higher filtering requirements High leakage current peaks
Limitations	Reduced efficiency in transformerless PV applications with full-bridge topology	Unsuitable in transformerless PV application with full-bridge topology due to high leakage current	Unsuitable in transformerless PV application with full-bridge topology due to high leakage current

5. CONTROL OF THREE-PHASE PV SYSTEMS

5.1. On-Grid PV Power Plant

The main control issues in the on-grid three-phase PV power plants include [12-13]:

- Management of the DC-link voltage: The DC voltage can be subjected to transient conditions arising from the variability of the power produced by the PV array. An increase in the produced power results in voltage overshoot while a decrease results in voltage undershoot. Thus, power changes in the output of the PV array results in variation of the dc-link voltage. The control of the dc-link voltage is often done via the control of the frontend DC-DC converter.
- MPPT of the operating point of the PV array to ensure operation at the highest efficiency in any operating condition.
- Control of AC voltage

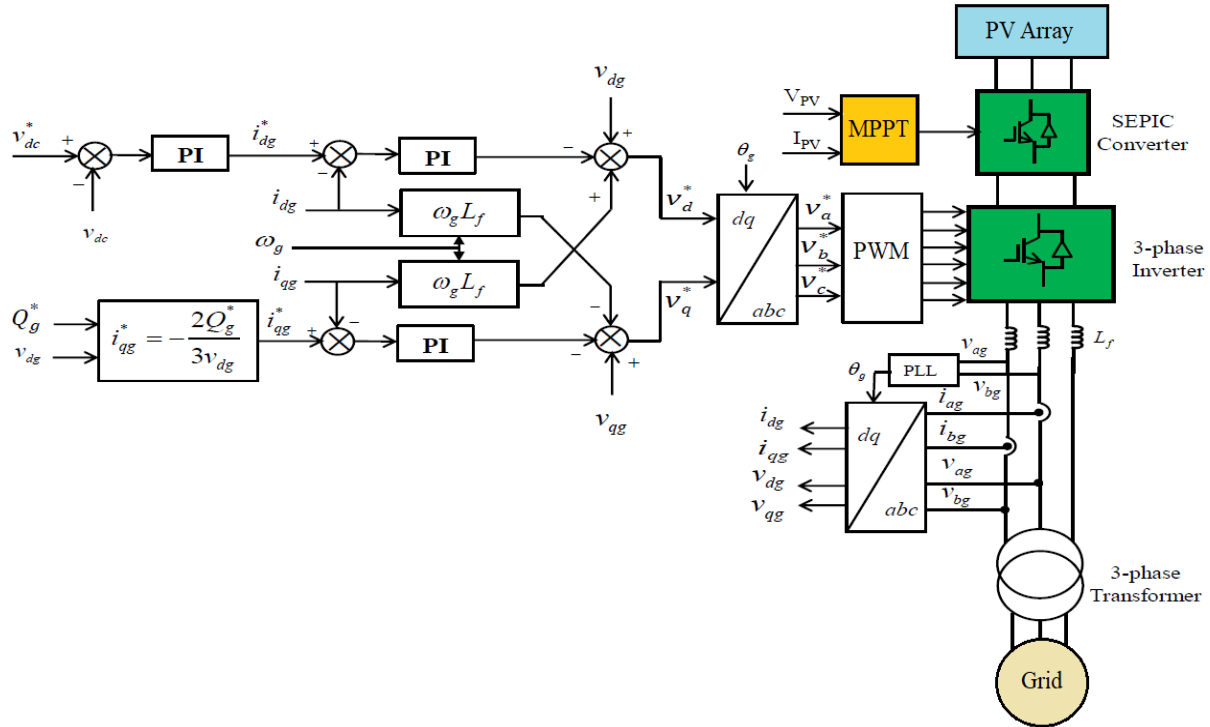


Fig. 8. Vector control scheme for a three-phase on-grid PV power plant.

- Control of AC current
- Grid synchronization
- Anti-islanding detection
- Grid monitoring

For such on-grid PV power systems, one of the most important considerations in the control of the inverter is the proper synchronization with the three-phase utility voltages. Such inverters interact with the grid at the point of common coupling (PCC) in order to attenuate voltage disturbances and reduce their undesirable consequences [13]. Moreover, such inverters are particularly sensitive to voltage disturbances which might affect the controllability of their control systems. For such inverters, proper three-phase synchronization can only be achieved with a well-designed control system since the three phases of a three-phase system do not work autonomously. Since in a balanced

three-phase system, the phases have equal amplitude, frequency and phase shifts, the synchronizations system should be able to detect any voltage vector disturbances. The control system of such an inverter should also be able to react to ride-through such operating conditions and the inverter partakes in supporting the grid frequency and voltage to ensure grid stability and safety. The vector control scheme of a grid-connected three-phase PV power plant for the control of grid side inverter is shown in Fig. 8. The control loops include [13, 14]:

- Two inner current control loops for the translated dq axis currents, i_{dg} and i_{qg} .
- One DC-link voltage control loop to regulate the DC-link voltage.
- Three-phase phase-locked loop (PLL).
- Maximum power point tracking (MPPT).
- Cross-feedback decoupled network.

The outer loops regulate the power flow of the system by controlling the active and reactive power injected into the grid. This is because of the dependence of the active and reactive powers on the direct and quadrature current components which are given as below [15]:

$$P_g = \frac{3}{2}(v_{dg}i_{dg}) = \frac{3}{2}|v_g|i_{dg} \quad (6)$$

$$Q_g = \frac{3}{2}(v_{dg}i_{qg}) = \frac{3}{2}|v_g|i_{qg} \quad (7)$$

The overall inductance (L_f), downstream with respect to the inverter has the following voltage balance:

$$\begin{bmatrix} v_{ag} \\ v_{bg} \\ v_{cg} \end{bmatrix} = R_f \begin{bmatrix} i_{ag} \\ i_{bg} \\ i_{cg} \end{bmatrix} + L_f \frac{d}{dt} \begin{bmatrix} i_{ag} \\ i_{bg} \\ i_{cg} \end{bmatrix} + \begin{bmatrix} v_{a1} \\ v_{b1} \\ v_{c1} \end{bmatrix} \quad (8)$$

where R_f is the overall line resistance; i_{ag} , i_{bg} and i_{cg} represent the line currents, while v_{a1} , v_{b1} and v_{c1} represent the inverter output voltages. In the control scheme of Fig. 8, the three-phase synchronous PLL, is used for the detection of the phase angle and amplitude of the grid voltage; while the PWM scheme is used for the modulation of the inverter. The cross-feedback decoupling network is used to cancel out the effect of oscillation at 2ω on the synchronous reference voltage of the PLL [13].

5.2. Off-Grid PV Power Plant

In this subsection, a three-phase PV power plant not connected to a main grid is considered. These types of plants are often

autonomous, isolated or in the form of a microgrid for the following reasons [5]:

- Far distance of the users from the grid, which makes the cost of grid extension prohibitive.
- Difficult terrain to the load center.
- Size of the load.

The main technical problem with such standalone plants is related to frequency and voltage magnitude control, since unlike in the on-grid system, synchronization is not an issue. The vector control structure for the inverter of a standalone three-phase PV power plant is shown in Fig. 9 with the decoupled current controllers. The control system consists of the output voltage controller, the DC-link voltage controller, the current controller, MPPT controller, and the PWM for the generation of the switching pulses. Proportional-Plus-Integral (PI) controllers are used for the regulation of the output voltage and currents. The outer loop is the voltage controller while the inner loop is current controller. The absence of the PLL is obvious since there is no grid for synchronization functionality.

6. PROPOSED CONTROL SYSTEM FOR THE PV INVERTER

This section discusses the control strategy proposed to meet power quality requirements (240 V, 50 Hz), for the single-phase voltage-source inverter. The control structure proposed is shown in Fig. 10, designed to achieve the following control objectives [23]:

- Synthesize a single-phase sinusoidal AC output voltage from the DC input from the PV array or from the battery bank.
- Control of the magnitude of the AC output voltage to achieve 240 V RMS.

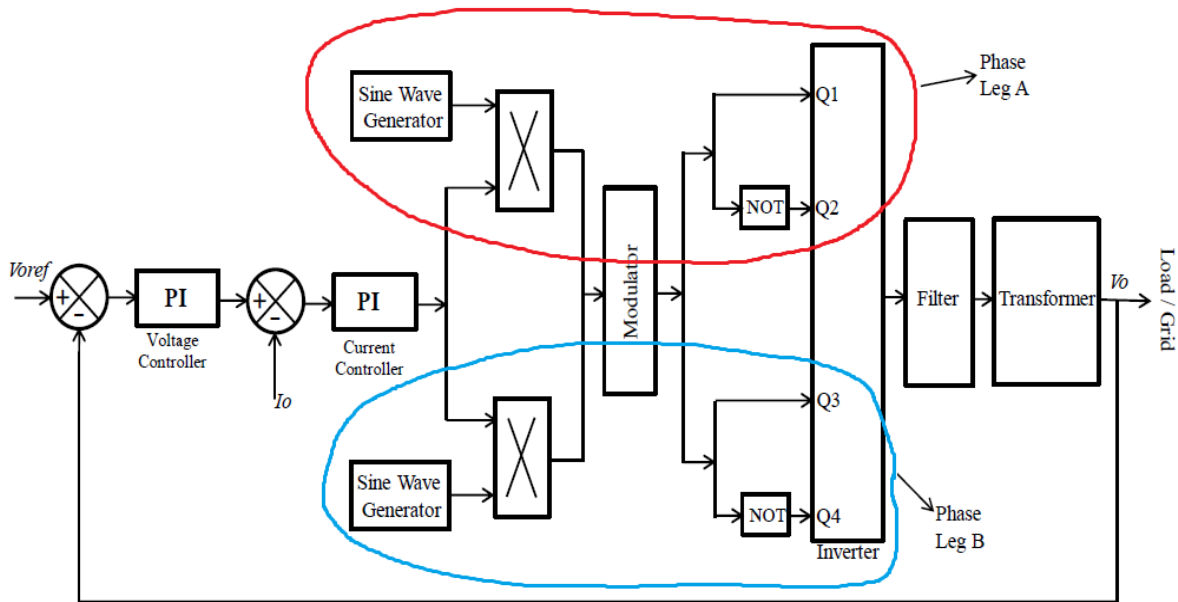


Fig. 10. Block diagram of the proposed control system for the single-phase inverter.

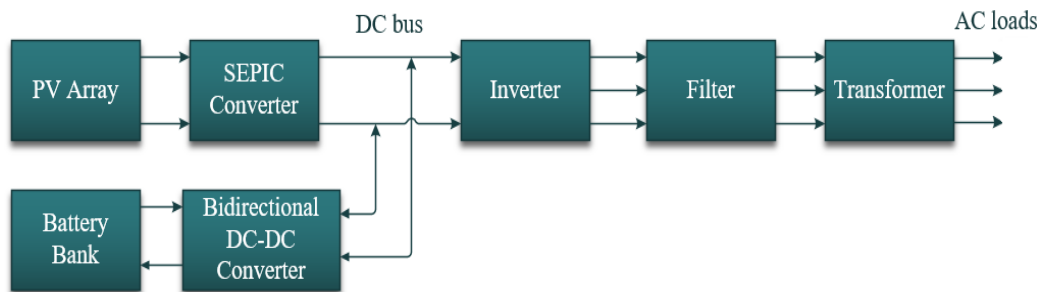


Fig. 11. Block diagram of the power circuit of the complete PV plant being modelled.

the low pass LC filter. The filter removes the higher frequency harmonics not removed by the modulation process. Finally, the output transformer with a transformation ratio of 1: 2 steps the voltage up to 240 V AC before utilisation by the load or before integration to the grid.

To investigate the behavior of the inverter and its performance in relation to the other subsystems, a simulation model is developed using MATLAB/Simulink software. Fig. 11 depicts the modelling of the other major subsystems of the complete PV power plant. Those models are now integrated with the

voltage-source inverter based on the H-bridge topology to realise the complete model of Fig. 12 which the PV array is the primary power source and generates a DC power. This is stepped up by the SEPIC converter to provide a DC-link voltage of 180 V. This voltage is used as input to the inverter and as a source for the bidirectional DC-DC converter to charge the energy storage system. The bidirectional DC-DC converter also operates during periods of low insolation or night time to discharge the battery bank which serves as a backup power supply. The LC filter which is integrated with

the transformer in the model filters out the high frequency harmonics generated from the switching action of the inverter. Since the 180 V of the DC-link is not enough to provide the needed AC output voltage of 240 V, the filtered output is stepped up by the line frequency transformer.

Fig. 12 also shows the various control blocks: MPPT for efficient extraction of PV energy; DC-link voltage regulator to ensure the DC voltage which is maintained at 180 V; battery bank manager which determines when the battery bank is to be charged or to be discharged; and inverter controller which implements the unipolar SPWM discussed in the previous section.

The controllers developed were used in simulation studies for both the single-phase operation and for three-phase operation in the standalone mode. For the single-phase operation, the results are shown in Figs. 13-15, while the results for the three-phase operation are shown in Figs. 16-19. The detailed discussions are presented below.

6.1. Single-Phase PV System

For the single-phase operation, at a step time of 1 second, a circuit breaker switches on a load of 3.5 kW into the system and switches it off at the step time of 1.5 seconds. The variation of the line frequency during the switching operation is shown in Fig. 13. It is

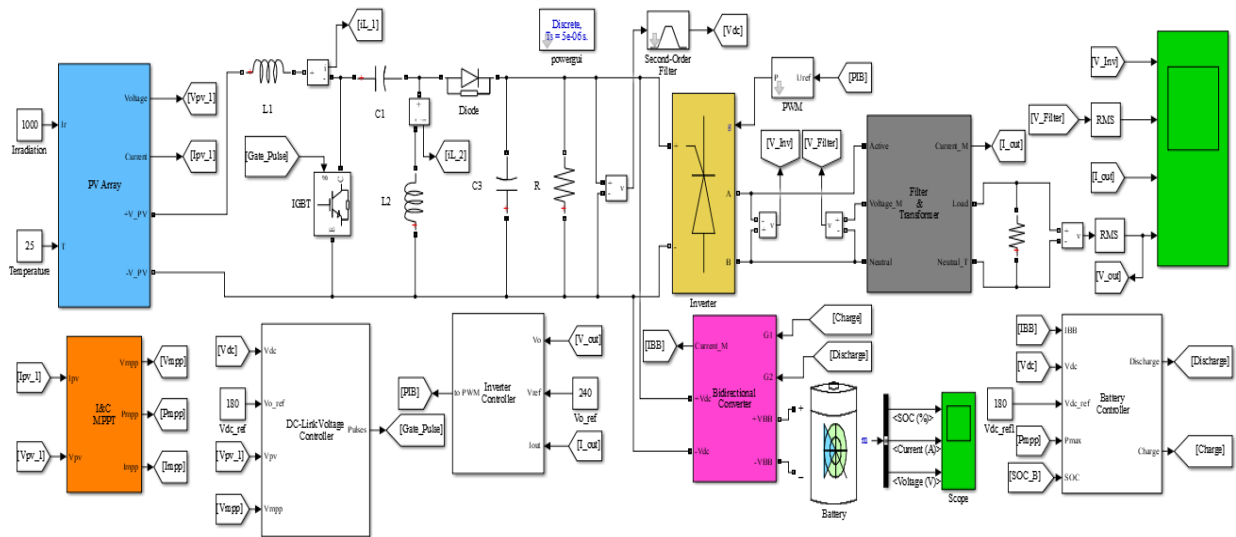


Fig. 12. The overall simulation model of PV system.

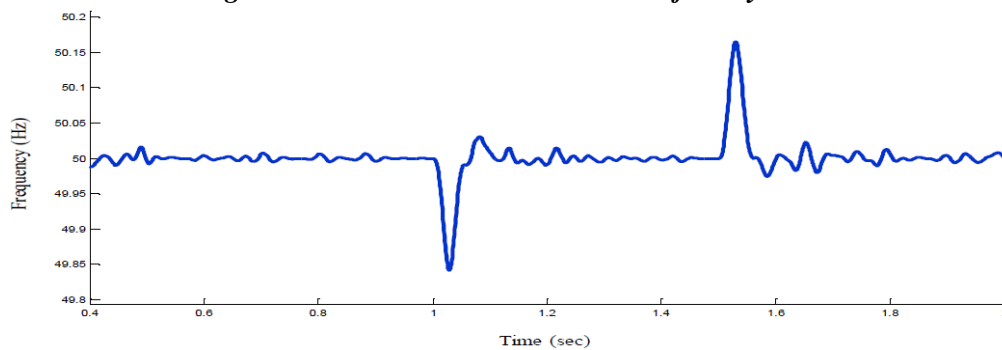


Fig. 13. Line frequency of the system during the switching operation.

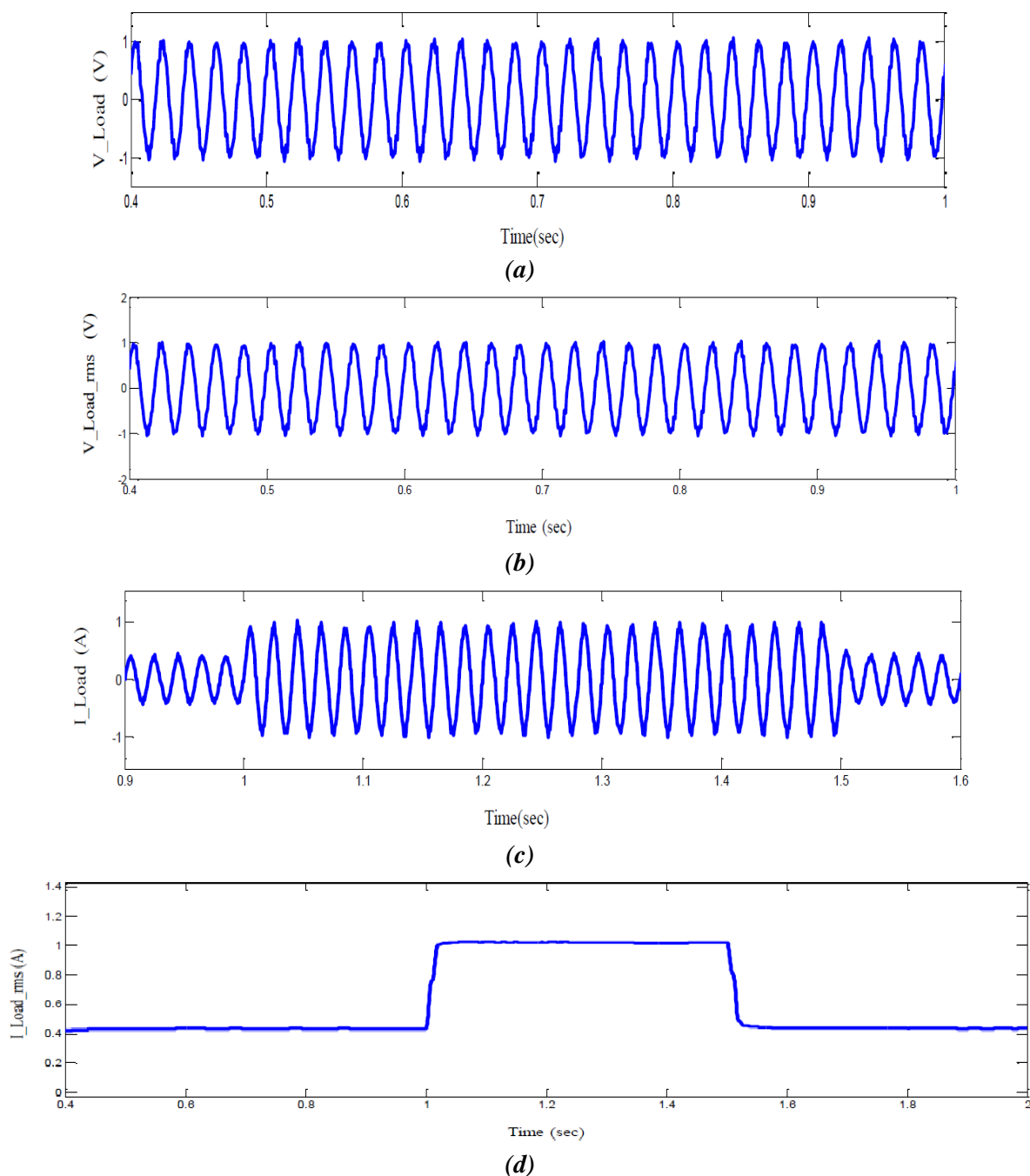


Fig. 14. Load voltages and currents during the switching operation, (a) instantaneous load voltage during operation, (b) the RMS load voltage during operation, (c) the instantaneous load current, and (d) the RMS load current.

observed that the frequency deviation from the nominal value of 50 Hz is minimal and within acceptable limits. The instantaneous

values and RMS values of the load voltages and currents during this switching operation are shown in Fig. 14 in per unit values. The

current transitions (increment and decrement) during the switching operation are obvious in Figs. 14(c) and 17(d). Also, it is shown in Fig. 15 the corresponding power flow during the switching operation. Fig. 16 shows the unfiltered single-phase voltage

waveform of inverter output and harmonic orders up to 10th rank. It can be found that even rank harmonics and the size of odd ones up the 10th rank have decreased below 5% of the fundamental harmonic order.

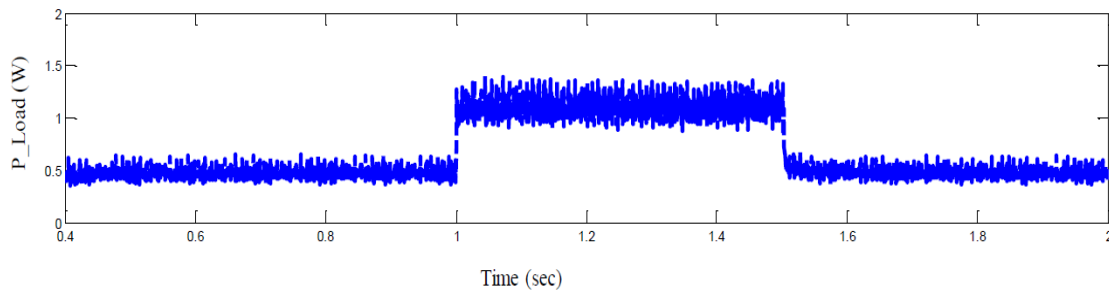


Fig. 15. Load power flow during the switching operation.

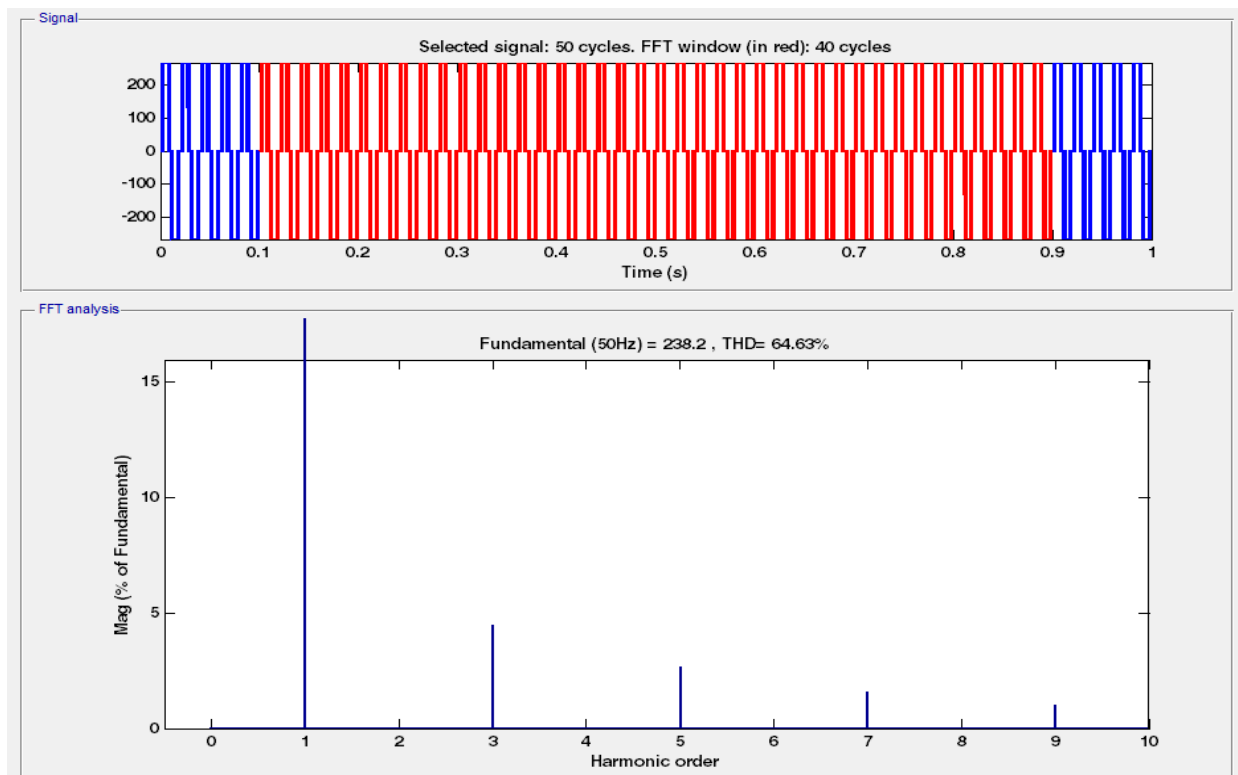


Fig. 16. Single-phase inverter output voltage THD.

6.2. Three-Phase Off-Grid PV System

For the three-phase system, Fig. 9, at a step time of 1 second a 3-phase load of 2.5 kW

is switched on, while an additional load of 3.5 kW is also switched on at a time of 1.5 seconds. The results for this double switching operation are shown in Figs. 17-21.

Fig. 17 shows the frequency deviations obtained. Like in the single-phase case, this is still maintained within the required limits. The instantaneous and RMS load currents in per units are shown in Fig. 18, with the current transitions at the switching times obvious. The power flow is shown in Fig. 19 while Fig. 20 is showing the three-phase

instantaneous load voltage. Fig. 21 shows the unfiltered three-phase voltage waveform of inverter output and harmonic orders up to 10th rank. It can be found that even rank harmonics and the size of odd ones up the 10th rank have decreased below 5% of the fundamental harmonic order.

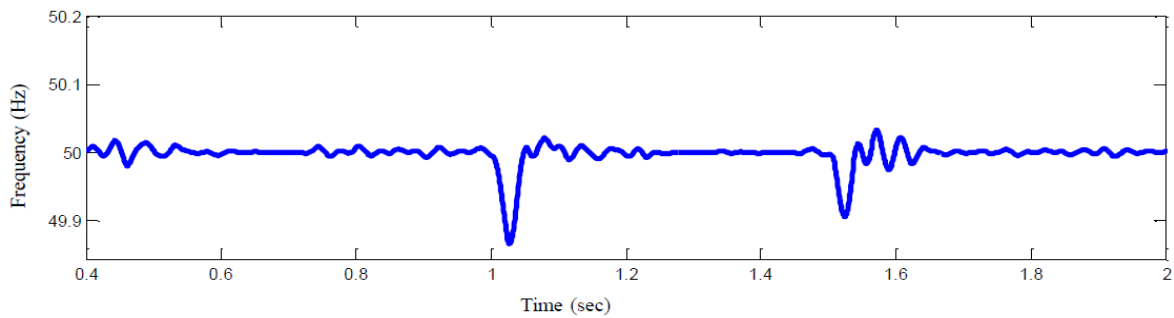
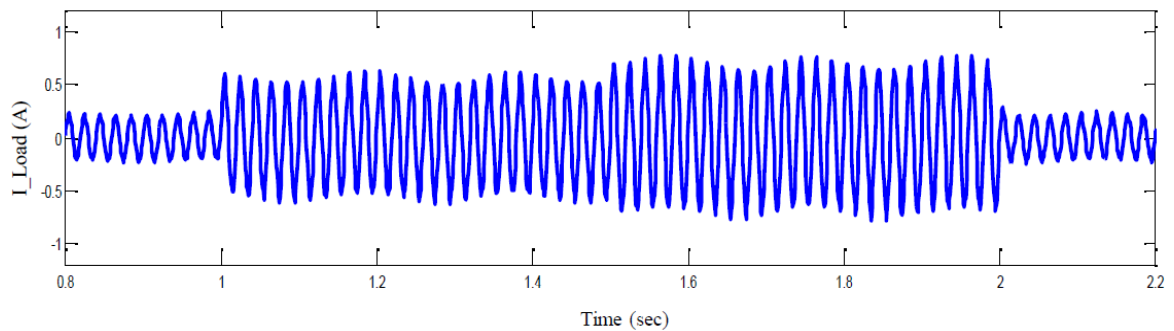
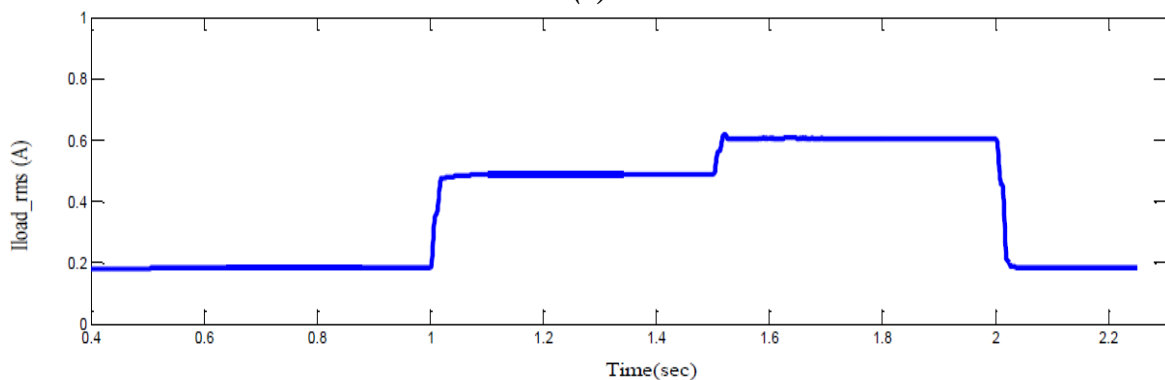


Fig. 17. Load frequency during three-phase operation.



(a)



(b)

Fig. 18. Load current changes during the switching operation, (a) the instantaneous load current in three-phase operation, and (b) the RMS load current.

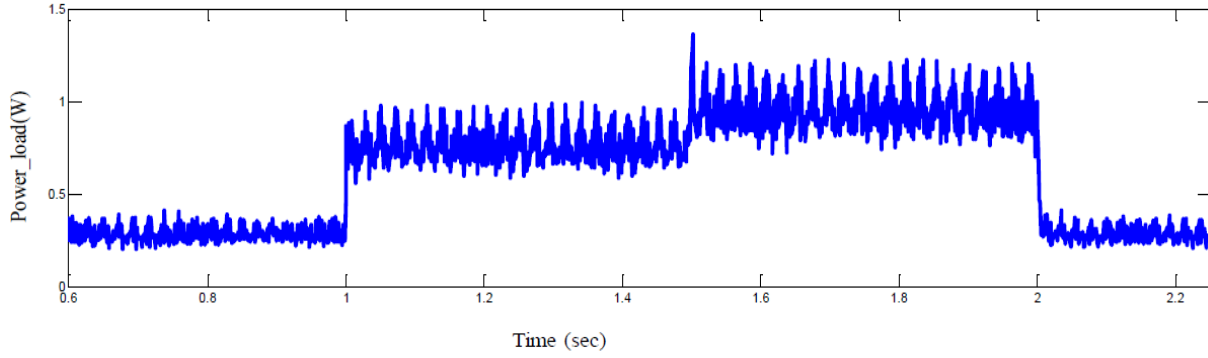


Fig. 19. Load power changes during the three-phase switching operation.

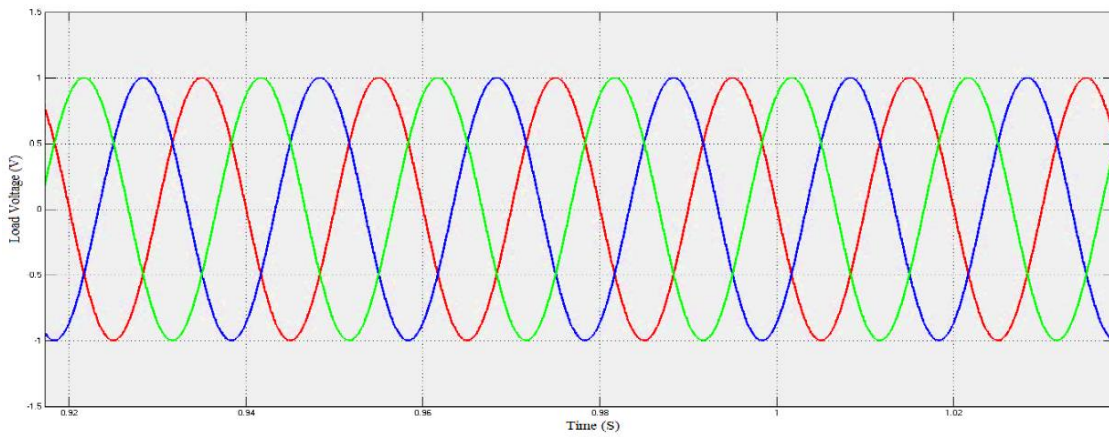


Fig. 20. Load voltage.

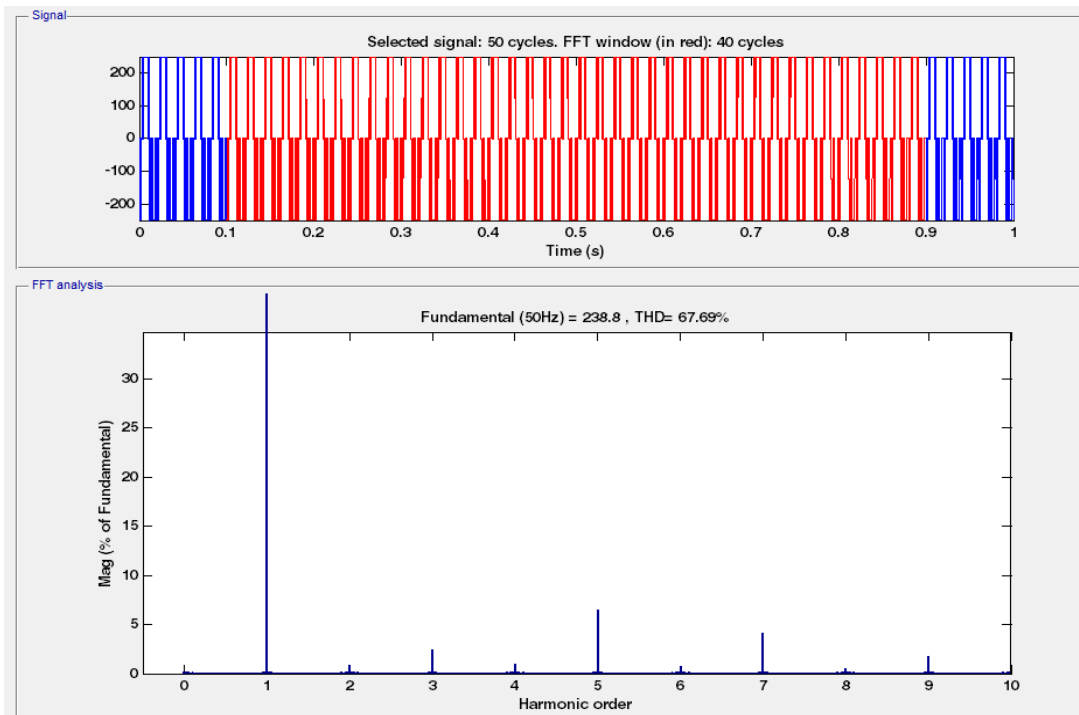


Fig. 21. Three-phase inverter output voltage THD.

7. CONCLUSION

The topologies and different modulating strategies of the H-bridge based PV inverters have been presented. A modulation scheme based on the unipolar SPWM technique has been proposed and used for the inverter switching operation. The simulation studies confirm the feasibility and effectiveness of the control strategy. The proposed control strategy is able to synthesise AC voltage from the DC voltage from the PV array or the backup battery energy storage system. It is evident that the control strategy is able to provide a sinusoidal output voltage with the harmonics reduced to the barest minimum after minimal filtering. Moreover, the robustness of the control system has been demonstrated by the ability of the system to maintain the load frequency and voltage magnitudes, in both single-phase and three-phase operations, within the required limits even in the events of changes in the system loading.

REFERENCES

- [1] Mukhtar Ahmad, Operation and Control of Renewable Energy Systems, 1st ed. John Wiley & Sons Inc: New York; 2017.
- [2] A. Keyhani, Design of Smart Power Grid Renewable Energy Systems, New Jersey: John Wiley & Sons, 2011.
- [3] Peddapelli, Satish Kumar.. Pulse Width Modulation. De Gruyter: Berlin; 2017.
- [4] W. Kramer, S. Chakraborty, B. Kroposki, and H. Thomas, Advanced power electronic interfaces for distributed energy systems. Part 1: Systems and topologies, National Renewable Energy Lab., Golden, CO, Tech. Rep. NREL/TP-581-42672, 2008.
- [5] P. Gevorkian, Grid-Connected Photovoltaic Power Generation: Technologies, Engineering Economics, and Risk Management. Cambridge University Press: Cambridge; 2017.
- [6] A. Khaligh, and O. C. Onar, Energy Harvesting: Solar, Wind, and Ocean Energy Conversion Systems, New York: Taylor & Francis Group, 2010.
- [7] F. Blaabjerg. Power Electronics in Renewable Energy Systems. Institute of Energy Technology, Aalborg University, Denmark. [Online]. Available:www.icit2010.usm.cl/doc/plenary/blaabjerg.pdf., 2010.
- [8] R. Gonzalez, J. Lopez, P. Sanchis, and L. Marroyo, Transformerless inverter for single-phase photovoltaic systems, IEEE Trans. Power Electronics, vol. 22, no. 2, pp. 693-697, 2007.
- [9] B. Gu, J. Dominic, J. Lai, C. Chen, T. Labella, and B. Chen, High reliability and efficiency single-phase transformerless inverter grid-connected photovoltaic systems, IEEE Trans. Power Electronics, vol.28, no. 5, pp. 2235-2245, 2013.
- [10] S.V Araujo, P. Zacharias, and R. Mallwitz, High efficient single-phase Transformerless inverters for grid-connected photovoltaic systems, IEEE Trans. Industrial Electronics, vol. 57, no. 9, pp. 3118-3128, 2010.
- [11] D.W. Hart, Power Electronics, McGraw-Hill, New York, 2011.
- [12] J. Olamaei, S. Ebrahimi, A. Moghassemi, Compensation of Voltage

-
- Sag Caused by Partial Shading in Grid-Connected PV System Through the Three-Level SVM Inverter, *Sustainable Energy Technology & Assessments*, vol. 18, pp. 107-118, 2016.
- [13] F. Blaabjerg, R. Teodorescu, M. Liserre, and A. V. Timbus, Overview of control and grid synchronization for distributed power generation systems, *IEEE Transactions on Industrial Electronics*, vol. 53, pp. 1398–1409, 2006.
- [14] S. Buso & P. Mattavelli, *Digital Control in Power Electronics*, Morgan & Claypool, Nebraska-Lincoln, USA, 2006.